Magn Reson Imaging Clin N Am
10 (2002) 237–251

MRI CLINICS OF NORTH AMERICA

Magnetic resonance imaging of mediastinal vessels

Ramiro J. Hernandez, MD

Department of Radiology, Section of Pediatric Radiology, C.S. Mott Children's Hospital F3503, University of Michigan Health System, 1500 East, Medical Center Drive, Ann Arbor, MI 48109-0252, USA

MRI complements echocardiography and cineangiography in the evaluation of the great vessels. Advantages of echocardiography are its low cost, ready availability, and portability. Similar to echocardiography, MRI is noninvasive and lacks ionizing radiation, but it also has the advantages of multiplanar imaging and large field of view. This article reviews the indications for MRI of the great vessels of the chest and the magnetic resonance (MR) appearance of some of the more common anomalies of the pulmonary arteries, aorta, and systemic and pulmonary veins.

MRI techniques

The thoracic vessels can usually be completely imaged with a T1-weighted spin-echo sequence followed by three-dimensional (3D) gadolinium-enhanced MR angiography. These sequences can be supplemented with a cine gradient-echo technique, using segmented k-space acquisition (Fastcard or Fastcine).

Spin-echo and cine gradient echo techniques including segmented k-space acquisition, safety considerations, and sedation requirements have been previously described [1]. Therefore, they will not be discussed in this article; however, a brief description of contrast-enhanced MR angiography, as it pertains to imaging children, will be discussed.

Contrast-enhanced MR angiography takes advantage of the T1 shortening property of paramagnetic agents (such as gadolinium chelates) and 3D imaging. The advantages of 3D gadolinium-enhanced MR angiography over other MRI techniques for the evaluation of the thoracic vessels include (a) rapid acquisition, (b) ability to image vessels in any plane, and (c) absence of a dephasing artifact. 3D gadolinium-enhanced MR angiography of the thoracic vessels in infants and young children is performed with a nonbreath-hold technique; in older children and adolescents, a breath-hold technique can be used. A double dose (0.2 mmol/kg body weight) of gadolinium suffices for optimal visualization of the mediastinal vessels [2].

Multiplanar volume reconstructions, as well as maximum intensity projections (MIP) and subvolume MIPs, are obtained in orthogonal and oblique plains to optimally display the vessel of interest.

Pulmonary arteries

Abnormalities of the pulmonary arteries often occur in association with obstructive lesions of the right ventricular outflow tract (eg, pulmonary artery atresia, stenosis, and hypoplasia), truncus arteriosus and its variants, and pulmonary sling.

Obstructive lesions of the pulmonary artery

Assessment of the arterial supply to the lungs is crucial for the management of children with congenital heart disease, especially those with obstructive lesions of the right ventricular outflow tract/pulmonary arteries. The arterial supply to the lungs can have a dual origin: the pulmonary arteries and aortopulmonary collateral vessels. Two-dimensional spin-echo or gradient echo imaging techniques usually suffice to depict the central pulmonary arteries [3]; however, gadolinium-enhanced MR angiography is required to adequately evaluate the hilar and intrapulmonary segments of the central pulmonary arteries and aortopulmonary collateral vessels (Fig. 1).

E-mail address: rjhm@umich.edu (R.J. Hernandez).

PII: S1064-9689(01)00011-3

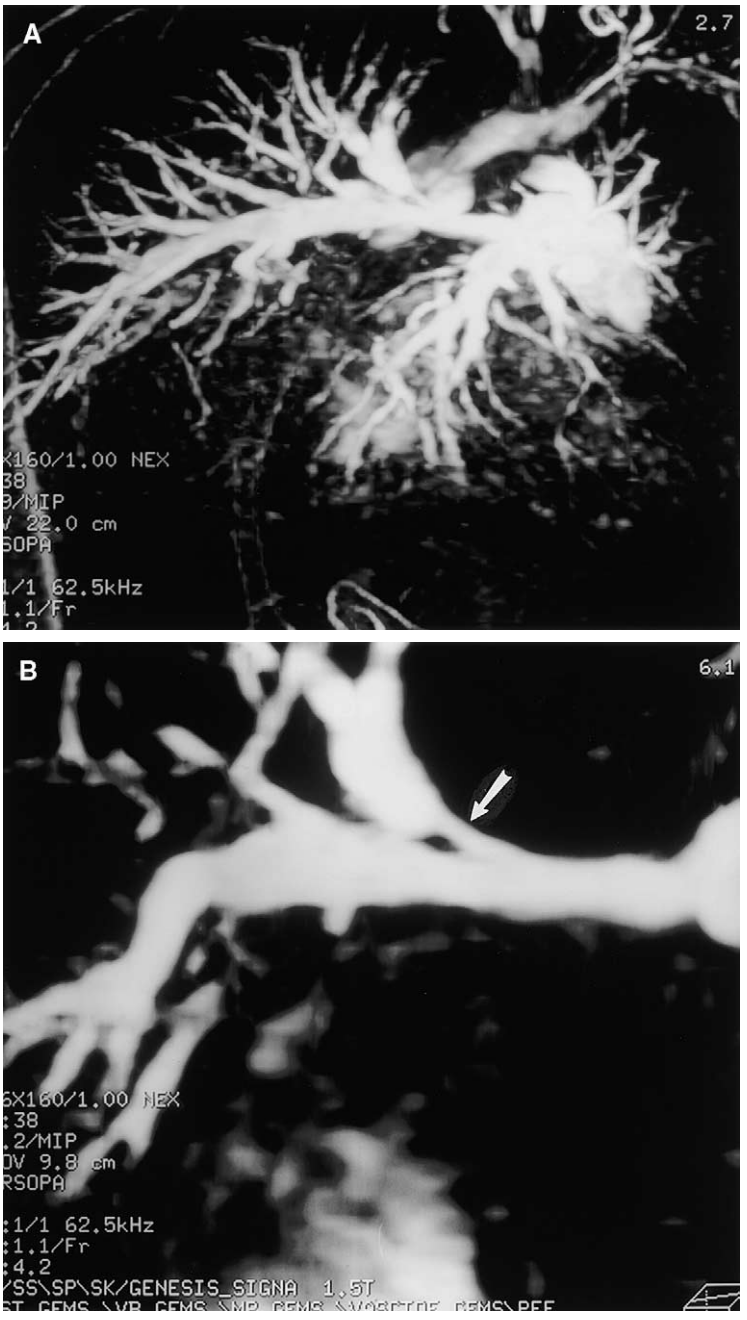

Fig. 1. Pulmonary artery stenosis in a 13-year-old boy with Williams syndrome. (A) Oblique-coronal reformatted image from a 3D gadolinium-enhanced MR angiogram demonstrating the right pulmonary artery and its branches. (B) Close-up of an oblique coronal reformatted image demonstrating stenosis of the right upper lobe pulmonary artery branch (*arrow*) with poststenotic dilatation.

In patients with obstructive lesions of the pulmonary artery, the presence, caliber, and confluence of the pulmonary arteries must be assessed. Although the hilar portions of the pulmonary arteries are always present, the central pulmonary arteries may be absent. Cineangiography is the gold standard for imaging the pulmonary arteries; however, right ventricular outflow obstruction and dilution of contrast by nonopacified blood (via shunts or collaterals) may impair opacification of the pulmonary arteries. Surgical and autopsy series have shown patency of the pulmonary arteries even though they were not seen by angiography, despite injections of contrast medium into the aorta, aortopulmonary collaterals, and pulmonary veins [4].

MRI can identify central pulmonary arteries not visualized by angiography [5,6]. The ability of MR to assess the size and confluence of the central pulmonary arteries in patients with obstructive lesions of the pulmonary outflow tract ventricular outflow is nearly equivalent to that of cine-angiography [6]; however, measurements of the caliber of these vessels on MR are slightly smaller than those acquired on cine-angiography. The interobserver and intraobserver variability of central pulmonary arteries size assessment is similar for MRI and angiography [6].

In patients with pulmonary atresia, it is important to assess the presence, origin, size, and distribution of the aortopulmonary collateral vessels (Fig. 2). The presence of stenosis in the collateral vessels and any anastomosis with the pulmonary circulation should also be evaluated. Aortopulmonary collateral vessels may originate from brachiocephalic arteries, from the descending thoracic aorta, or from the subdiaphragmatic aorta. These collateral arteries often have an asymmetric distribution within the various lobes of the lungs, and they can anastomose with intrapulmonary vessels. Therefore, some bronchopulmonary segments may have dual or multifocal arterial supply from the pulmonary arteries, and also from aortopulmonary collateral vessels. Other bronchopulmonary segments may have only a solitary supply, either from true pulmonary arteries or from the aortopulmonary collateral circulation. The best MR technique to evaluate the aortopulmonary collateral vessels is 3D gadolinium-enhanced angiography, because it allows reformatting in any plane, essential for delineating the often-tortuous collateral vessels.

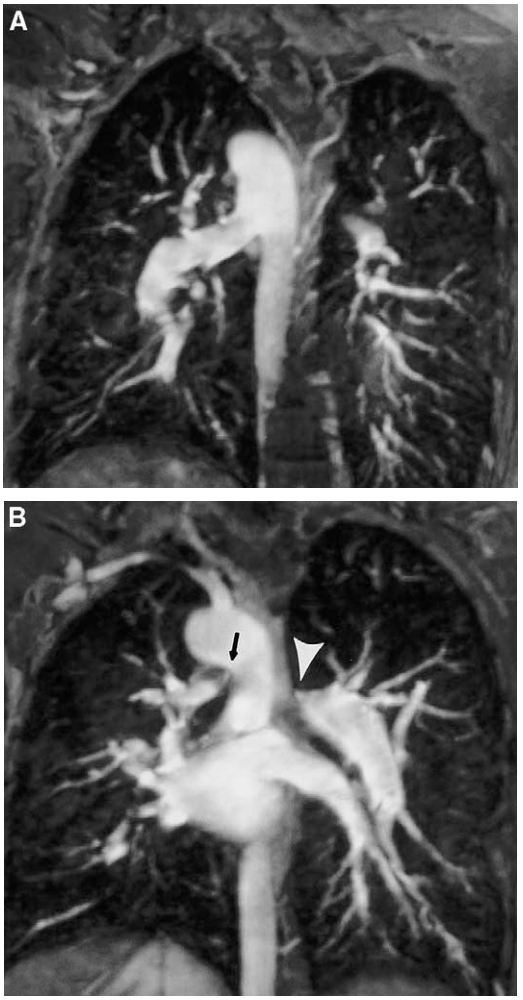

Fig. 2. Pulmonary atresia and ventricular septal defect in a 20-year-old woman. (A) Coronal reformatted image from a 3D gadolinium-enhanced MR angiogram demonstrating large collateral vessel originating from the descending thoracic aorta supplying the lower two thirds of the right lung. (B) Coronal reformatted image slightly more anterior to (**A**) showing two collateral vessels supplying the right upper lung (*arrow*) and the left lung (*arrowhead*) originating from the descending thoracic aorta.

Truncus arteriosus

The pulmonary arteries can arise from the aorta in some types of congenital heart disease, such as truncus arteriosus and hemitruncus. In truncus arteriosus a single vessel originates from the base of the heart and gives origin to the coronary, pulmonary, and systemic arterial circulations. Between 5% and 10% of patients with

Fig. 3. Aortopulmonary window T1-weighted spin-echo coronal section shows absence of the septum between the aorta and the pulmonary artery.

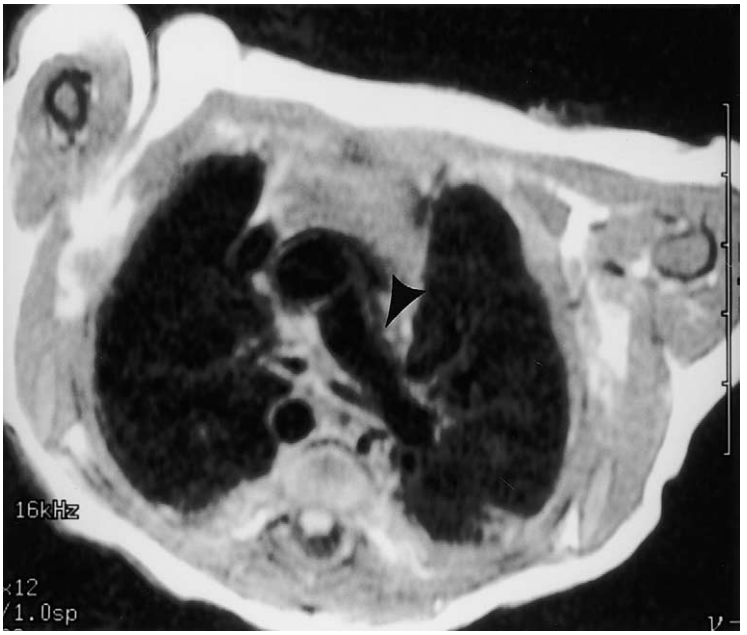

Fig. 4. Hemitruncus. T1-weighted spin-echo axial section of the chest. The left pulmonary artery (*arrowhead*) originates from the ascending aorta. The right pulmonary artery originated from the right ventricle.

truncus arteriosus will have absence of one of the pulmonary arteries, usually the left pulmonary artery. Truncus arteriosus must be distinguished from an aortopulmonary window, where an anomalous communication between the main pulmonary artery and the aorta exists (Fig. 3); however, two semilunar valves are present. In hemitruncus, one of the pulmonary arteries originates from the ascending aorta. The anomalous pulmonary artery arises from the proximal half of the ascending aorta; in most cases the abnormal vessel is the right pulmonary artery (Fig. 4).

Pulmonary sling

In patients with pulmonary sling, the left pulmonary artery originates from the right pulmonary artery, crossing the mediastinum from right to left between the trachea and esophagus (Fig. 5). Children with pulmonary artery sling typically present with respiratory symptoms due to compression of the airway by the left pulmonary artery or associated stenosis of the trachea or main bronchi. The abnormal anatomy is easily seen on axial imaging studies, including MRI and CT, although the relationship between the anomalous vessel and the esophagus and trachea is sometimes difficult to appreciate through cineangiography.

Aorta

MRI is useful in evaluation of vascular rings, nonvalvar stenosis of the aorta (eg, coarctation, interrupted arch, supravalvular stenosis), and aneurysm formation.

Vascular rings

Vascular rings result from an abnormal development of the aortic arch system, which results in derivatives of the arch encircling the trachea and esophagus. The effects of a vascular ring on surrounding structures can usually be detected through chest radiography and a contrast esophagram. When airway symptoms, tracheal compression on the chest radiograph, and characteristic indentation of the esophagus on the esophagram are present, no further imaging is needed. Additional imaging (CT or MR) is required when radiographic or clinical findings are not diagnostic [7] or when further definition of the anatomy is required for surgical planning. MRI in the axial plane as well as in coronal images is most useful in demonstrating the precise anatomy of suspected or known vascular rings.

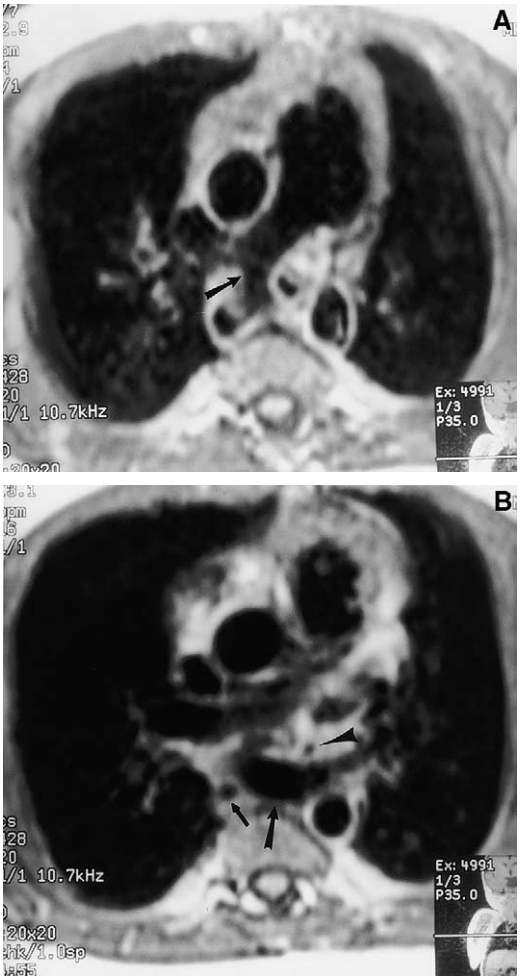

Fig. 5. Pulmonary sling. T1-weighted spin-echo axial sections. (A) The origin of the left pulmonary artery from the right pulmonary artery (*arrow*) can be clearly seen. (B) The left pulmonary artery (*large arrow*) courses between the stenotic trachea (*arrowhead*) and the esophagus (*small arrow*).

The common symptomatic vascular rings are the double aortic arch and the right aortic arch with an aberrant left subclavian artery. In a double aortic arch, both aortic arches may be patent, or one of them may be atretic, usually the left arch. Although the right arch tends to be higher and larger than the left, occasionally the left may be the dominant one (Fig. 6). When the vascular ring is secondary to a right aortic arch with an aberrant left subclavian artery, the aberrant subclavian artery originates from an aortic diverticulum (Kommerell diverticulum), and the vascular ring is completed by the ligamentum arteriosum.

Fig. 6. Double aortic arch. T1-weighted spin-echo axial section of the chest. Although the right arch is usually the dominant one, in this patient the left arch is dominant.

The length of the ligamentum arteriosum determines the presence or absence of symptoms.

Nonvalvar stenosis of the aorta

Coarctation of the aorta

Coarctation of the aorta refers to a congenital anomaly of the aorta characterized by a constriction or obliteration of a section of that vessel. Although the constriction of the aortic lumen can occur anywhere in the aorta, the most frequent site of constriction is immediately below the origin of the left subclavian artery at the insertion of the ductus arteriosus or ligamentum arteriosum. The basic pathologic lesion is a juxtaductal indenta-

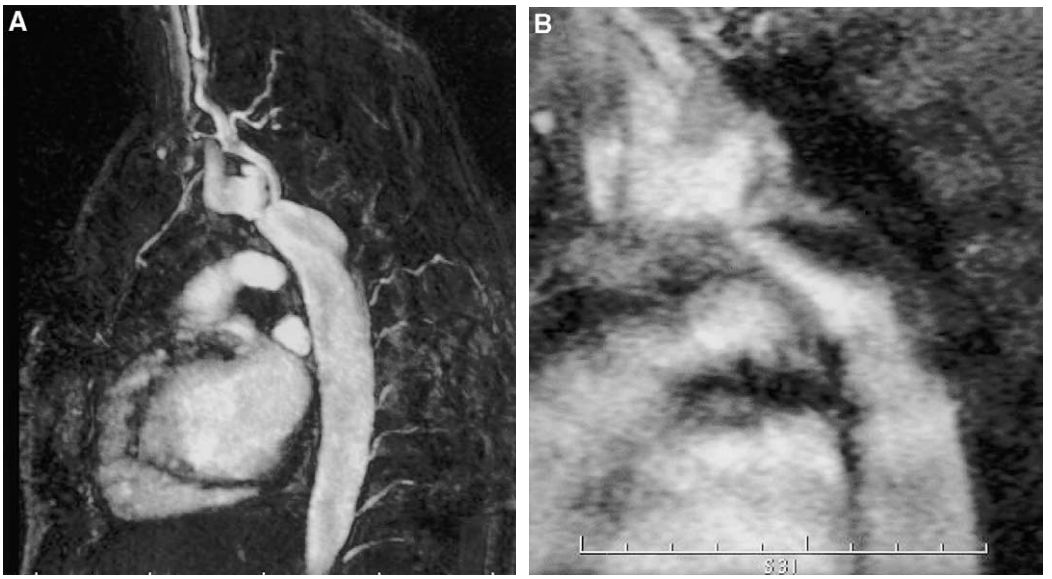

Fig. 7. Coarctation of the aorta. (A) Oblique sagittal reformatted image from a 3D gadolinium-enhanced MR angiogram demonstrating a discrete area of coarctation proximal to the origin of the left subclavian. (B) Oblique sagittal Fastcine image through the area of coarctation demonstrates turbulent flow, seen as a black jet, at the coarctation site.

tion, or "shelf", involving the posterior wall of the aorta. Less frequently, the narrowing may involve a long segment of the transverse aortic arch, usually associated with discrete narrowing at the isthmus. A reliable diagnosis of coarctation can usually be made through physical examination, chest radiography, and echocardiography. Additional diagnostic imaging may be needed in patients with suspected coarctation of the aorta when other noninvasive modalities fail to demonstrate the site and extent of the coarctation.

In MRI, coarctation of the aorta usually appears as a discrete area of narrowing distal to the left subclavian artery, with or without accompanying hypoplasia of the aortic arch or isthmus [8] (Fig. 7); however, long segment coarctations or coarctations at sites other than the juxtaductal region occur (Fig. 8). Knowledge of the length and site of the coarctation is useful for therapeutic management of these patients. Balloon dilatation is not recommended in patients with long segment coarctations. MRI can be used to select patients suitable for balloon dilatation.

Coarctation of the aorta must be differentiated from pseudocoarctation. The characteristic appearance of pseudocoarctation is that of a long aortic arch with a kink occurring at the aortic isthmus distal to the origin of the left subclavian without significant narrowing of the lumen. The blood pressures in the upper and lower extremities are nearly always normal, although minor differences have been reported. There is no collateral circulation.

MRI is valuable in demonstrating aneurysms and restenosis after surgical repair or post balloon angioplasty [9,10]. Patients who have had repair of coarctation using prosthetic patches have an approximately 25% risk of developing aneurysms at the coarctation repair site [11].

In patients with aortic coarctation, identification of collateral flow is important for two reasons. First, it can help plan operative repair. If there are insufficient numbers of collateral vessels,

Fig. 8. Coarctation. Oblique sagittal reformatted image from a 3D gadolinium-enhanced MR angiogram demonstrating a long-segment coarctation of the aorta.

cross-clamping of the aorta may be contraindicated because it can result in spinal cord ischemia. Second, the extent of collateral vessel formation can indicate the severity of the narrowing. The larger the number of collaterals, the more likely that the coarctation is clinically significant. The diagnosis of collateral blood flow formation is based on: (a) visualization of collateral vessels bridging the area of aortic stenosis and merging into the descending aorta (Fig. 9) and (b) the presence of caudal flow in the collateral vessels on phase contrast imaging [12]. Quantitative assessment of collateral blood flow is done by velocity-encoded cine MRI. In patients with hemodynamically significant coarctation of the aorta, the normal flow pattern in the aorta is reversed. Normally, flow decreases in the descending aorta; however, increased inflow is observed when there is collateral circulation via the intercostal arteries. Assessing the contribution of collateral circulation to total flow allows for an estimate of the obstruction's severity [13].

Fig. 9. Coarctation with collateral vessel formation. Oblique sagittal reformatted image from a 3D gadolinium-enhanced MR angiogram demonstrating a discrete constriction of the aorta at the juxtaductal region. Multiple collateral vessels can be seen.

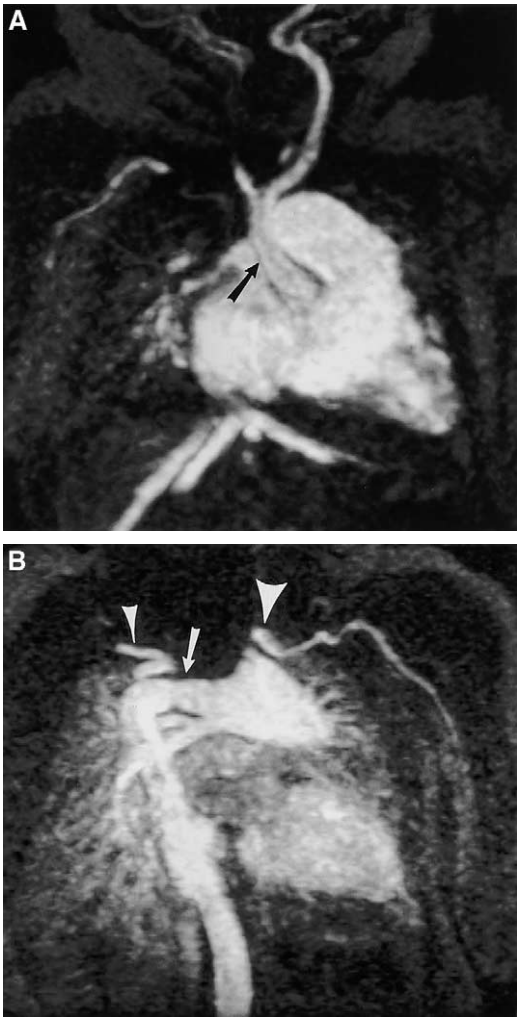

Fig. 10. Interrupted right aortic arch. Coronal reformatted images from a 3D gadolinium-enhanced MR angiogram of three-day old infant. (A) A small ascending aorta (*arrow*) is visualized to the right of a larger main pulmonary artery. (B) A large patent ductus arteriosus (*arrow*) connects the main pulmonary artery to the descending aorta on the right side of the spine. The left subclavian artery originates from the main pulmonary artery (*large arrowhead*), while the right subclavian artery originates from the proximal descending aorta (*small arrowhead*).

Interruption of the aortic arch

A lesion that is related to coarctation of the aorta is interruption of the aortic arch. This rare anomaly is characterized anatomically by complete discontinuity between the ascending and the descending aorta. It has been classified into three types:

Fig. 11. Takayasu arteritis. (A) Axial T1-weighted spin-echo axial section demonstrates marked thickening of the wall of the ascending and descending aorta (*arrows*). (B) Sagittal T1-weighted spin-echo axial section demonstrates decreased caliber of the ascending aorta.

Type A: interruption of the aortic arch distal to the left subclavian artery (42% of cases).
Type B: interruption of the arch between the left common carotid artery and the left subclavian artery (53% cases).
Type C: interruption of the arch proximal to the left carotid artery (5% of cases).

MRI can demonstrate the absent transverse arch and the patent ductus arteriosus supplying the descending aorta (Fig. 10). The patent ductus arteriosus should not be confused with the transverse arch.

Supravalvar aortic stenosis

Long segments of aortic narrowing can be seen in patients with various forms of arteritis, such as Takayasu arteritis or Williams syndrome. Takayasu arteritis is a primary arteritis of unknown origin that commonly affects the aorta and its major branches as well as the pulmonary artery. Although it is more commonly seen in Asian populations, the disease has a worldwide distribution. It usually affects young women, and its prevalence in female patients is about 10 times greater than that in male patients.

Williams syndrome is characterized by the coexistence of supravalvar aortic stenosis, peripheral pulmonary arterial stenosis, mental retardation, and a peculiar "elfin facies". Most commonly, supravalvar aortic stenosis occurs in association with the other features of Williams syndrome; however, the supravalvar aortic stenosis and peripheral pulmonary arterial stenosis can occur as isolated features, especially in the familial and sporadic forms of the syndrome. Some family members may also have supravalvar pulmonic stenosis, either as an isolated lesion or in combination with the supravalvar aortic anomaly. MRI can delineate the site and length of the aortic narrowing; when an arteritis is present, it can show the thickened arterial wall. The thickened arterial wall can only be seen on spin-echo sequences (Fig. 11).

Aneurysms and dissections of the aorta

Aortic aneurysms and associated dissections are rare in children. When seen in this age group, they are usually associated with predisposing conditions, such as Turner syndrome, coarctation of the aorta, Marfan syndrome, Ehlers-Danlos syndrome, Kawasaki disease, prior surgery, or trauma.

The size and extent of aortic aneurysms are clearly and accurately delineated by a combination of T1-weighted spin-echo, fastcard, and 3D gadolinium-enhanced MR angiography (Fig. 12). Although an aneurysm diagnosis is usually made by visual inspection, it is sometimes difficult to determine whether an area of aortic dilatation represents simple dilatation or an aneurysm. One guideline for distinguishing dilatation from aneurysm is that an aneurysm is present when the diameter of the aorta is greater than 50% of its normal diameter; however, this guideline can be difficult to apply, since data on the size of the aorta for different ages are not available. Another guideline is that an aneurysm is present when the aortic diameter of the proximal descending aorta is 1.5 times the diameter of the descending thoracic aorta at the level of the diaphragm [11].

MRI can be used to monitor aortic size in patients at risk for aneurysm formation (such as Marfan syndrome, Ehlers-Danlos syndrome, and

Fig. 12. Mycotic pseudoaneurysm in a two-year-old boy. Reformatted image from a 3D gadolinium-enhanced MR angiogram shows focal dilatation at the site of repair of a prior coarctation.

Fig. 13. Kawasaki disease. Reformatted image of a 3D gadolinium-enhanced MR angiogram demonstrating multiple aneurysms involving the brachial, brachiocephalic, iliac, and lumbar arteries. Aneurysms involving the coronaries, radial and popliteal arteries were also revealed. (*From* Hernandez RJ. Syllabus special course in pediatric radiology. Oak Brook, IL: Radiological Society of North America; 1999. p. 103–14; with permission.)

Kawasaki disease) because it can survey large areas. Traditionally, angiography had been used to follow these patients; however, this technique is not ideal in children because of its invasive nature and the risk of radiation exposure. Because MRI is noninvasive and does not utilize ionizing radiation, it has virtually replaced angiography in the serial assessment of patients who are at risk for aneurysm formation (Fig. 13).

Aortic dissection occurs when the intima and adventitia are separated from the media. It usually occurs at the junction between the middle and outer third of the media. The dissection may involve a localized area or the entire circumference of the aorta. The Stanford classification separates aortic dissections into two types: those affecting the ascending aorta (type A), which require emergency surgery, and those affecting only the descending aorta (type B), which can be managed medically. Dissections limited to the ascending aorta may be associated with cystic medial necrosis (with or without Marfan's syndrome).

Since aortic dissection is rare in children, no cumulative experience exists regarding the effectiveness of MRI in the evaluation of aortic dissection in children. Based on the experience reported in adult populations, 3D dynamic gadolinium-enhanced MR angiography is particularly useful for the evaluation of the aorta beyond the aortic valve (Fig. 14). Fastcard and spin-echo sequences provide an assessment of the sinus of Valsalva. After an aortic dissection is diagnosed, the extent and relationship of the dissection to

Fig. 14. Aortic dissection of a two-week-old infant who had undergone a previous balloon valvuloplasty for aortic stenosis. Sagittal reformatted image from a 3D gadolinium-enhanced MR angiogram shows a dissection extending from the level of the aortic arch to the midabdominal aorta.

the branch vessels should be determined, and the true lumen must be differentiated from the false lumen. Generally, the true lumen is smaller than the false lumen, has an oval shape, hugs the inner curve of the aorta, and contains faster-flowing blood. The false lumen is generally larger than the true lumen, is crescent-shaped, follows the outer curve of the aorta, and contains slower-flowing blood. Aortic cobwebs, representing fragments of media, can occasionally be seen in the false lumen. High pressures within the false lumen can increase its size and cause compression of the true lumen.

Multiplanar reformation of the 3D contrast-enhanced angiographic data provides a detailed display of the relationship of the origins of the branch vessels to the true and false lumens. Furthermore, these reconstructions can clearly depict extension of the dissection into the branch vessels and also locate sites of communication between true and false lumen, representing entry and reentry tears.

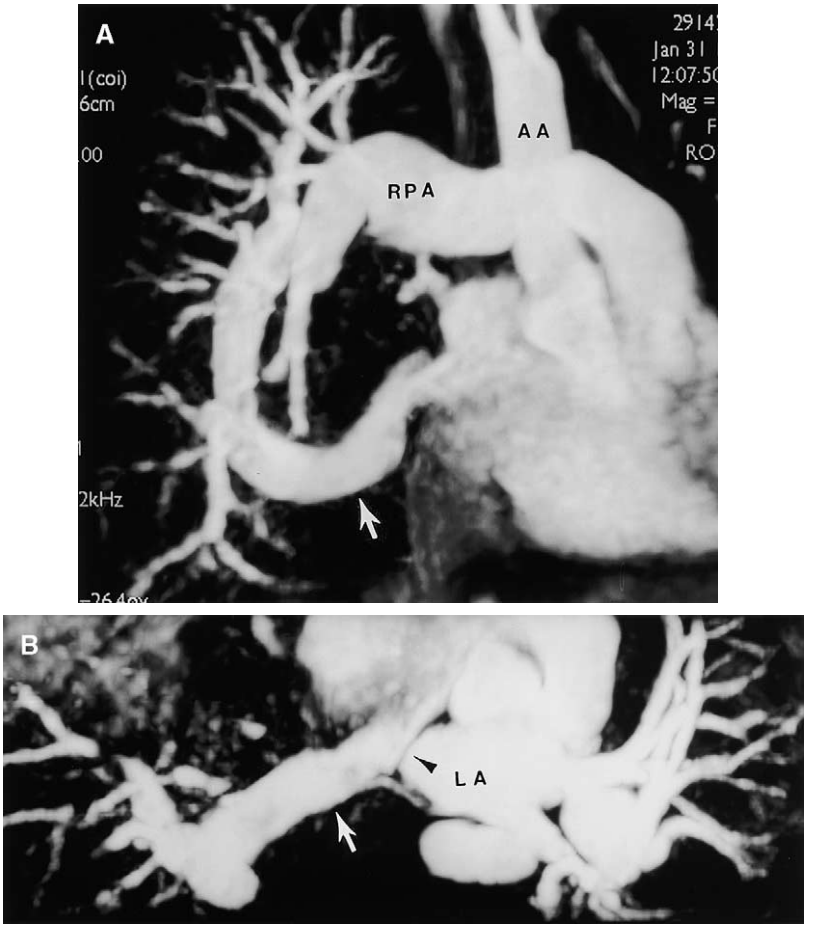

Fig. 15. Partial anomalous venous return. Patient had undergone a previous surgical correction. Because of the persistence of symptoms, 3D gadolinium-enhanced MR angiography was performed. (A) Oblique reformatted image showing a large pulmonary vein (*arrow*) draining almost the entire right lung. **AA** = ascending aorta; **RPA** = right pulmonary artery. (B) Axial reformatted image demonstrating persistent connection of the anomalous vein to the right atrium. The anomalous vein (*arrow*) enters to the right of the atrial septum (*arrowhead*). **LA** = left atrium. (C) Coronal reformatted image demonstrating small right pulmonary vein (*arrow*) draining to the left atrium (**LA**). (*From* Hernandez RJ. Syllabus special course in pediatric radiology. Oak Brook, IL: Radiological Society of North America; 1999. p. 103–14; with permission.)

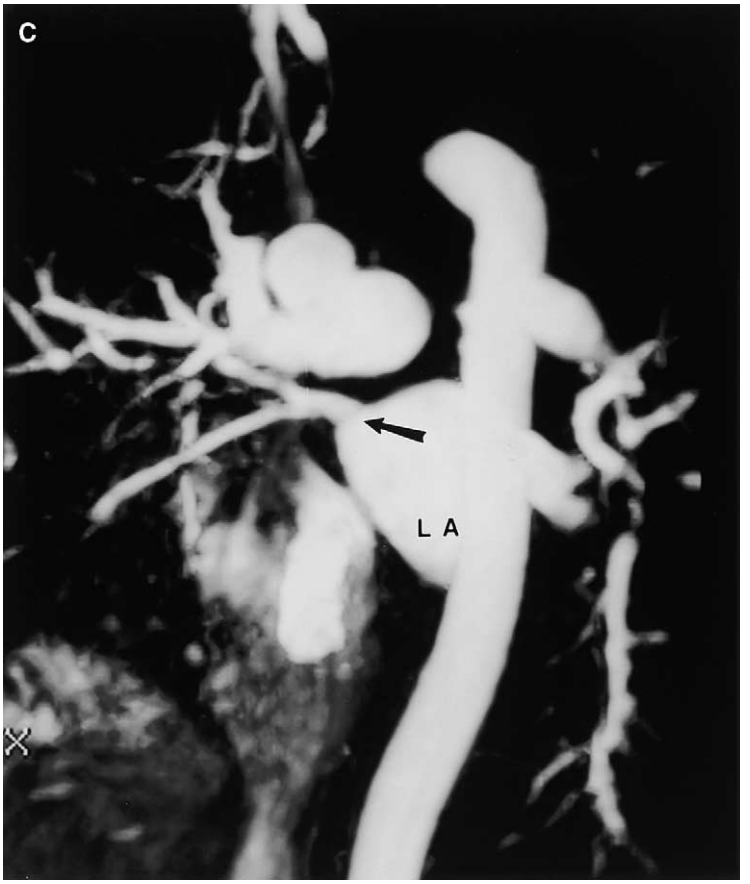

Fig. 15 (*continued*)

Systemic and pulmonary veins

Systemic veins

MRI can readily show the venous anatomy of the thorax and upper abdomen. Venous anomalies can be isolated or associated with congenital heart lesions, asplenia, and polysplenia. MRI complements echocardiography in the anatomic and hemodynamic evaluation of cardiac heterotaxia in infants and children [14,15], providing good visualization of both intracardiac and extracardiac structures; however, it is superior to echocardiography in the ability to delineate the systemic and pulmonary venous structures. In addition, it can provide useful information about abdominal situs (including splenic status), bronchial anatomy, relationship of the pulmonary arteries to the bronchi, and the morphology of both atrial appendages.

Polysplenia syndrome is characterized by an interruption of the inferior vena cava with azygous or hemiazygous continuation. The segment of the inferior vena cava between the liver and renal veins is absent and either the hemiazygous or azygous vein acts as a collateral vessel, ascending into the thorax in a retrocrural location. There is separate drainage of the hepatic veins into the right atrium via a common hepatic vein. The two main bronchi are long and hyparterial. In asplenia, the inferior vena cava and aorta are on the same side of the spine and course together in a piggy-back fashion to the site where the inferior vena cava enters the right atrium. Absence of the spleen and the presence of bilateral eparterial short main bronchi are findings that can be easily documented by MRI.

Other systemic venous abnormalities that can be diagnosed through MRI include persistence of the left superior vena cava, prominent left superior intercostal vein, anomalous left innominate vein, left inferior vena cava, duplication of the inferior vena cava, and thrombosis of the

superior vena cava. Determination of the presence of a persistent left superior vena cava is particularly important information in patients being considered for the Fontan operation [16].

Pulmonary veins

MRI can reliably demonstrate total or partial anomalous pulmonary venous return (Fig. 15). Compared with echocardiography and cardiac angiography, MRI is more accurate in the diagnosis of anomalous pulmonary venous connections [17,18]. Although a combination of 2D axial and coronal imaging can reveal most anomalous pulmonary veins, 3D gadolinium-enhanced MR angiography with its multiplanar capability allows optimal visualization of the pulmonary veins. MRI can also identify obstruction of the pulmonary veins [19].

Summary

Advances in technology have led to a changing role for MRI in the evaluation of the thoracic vasculature in children. MRI, especially with 3D gadolinium-enhanced MR angiography, can clearly demonstrate the morphology of the aortic and pulmonary vascular supply. In patients with nonvalvar obstructive lesions of the aorta (ie, coarctation, interruption of the aortic arch, and supravalvar stenosis), MRI can reliably assess the site and extent of the obstruction. Similarly, MRI can depict the morphology of the central pulmonary arteries and aortopulmonary collateral vessels in patients with obstructive lesions of the pulmonary artery. MRI is also useful in assessing the course of the aorta and pulmonary arteries in patients with suspected vascular rings. The result is that MRI can supplement information obtained from echocardiography and angiography and reduce the need for angiography.

References

[1] Hernandez RJ. Cardiovascular MRI. In: Siegel MJ, editor. MRI Clinics of North America. Philadelphia: W.B. Saunders Co.; 1996. p. 615–636.

[2] Hernandez RJ, Strouse PJ, Londy FJ, Wakefield TW. Gadolinium-enhanced MR angiography (Gd-MRA) of thoracic vasculature in an animal model using double dose gadolinium and quiet breathing. Pediatr Radiol 2001;31:587–593.

[3] Hernandez RJ, Rocchini AP, Bove EL, Chenevert TL, Gubin B. MRI of surgically created pulmonary artery narrowing in the dog. Pediatr Radiol 1989; 20:52–6.

[4] Presbitero P, Bull C, Haworth SCR, deLeval MR. Absent or occult pulmonary artery. Br Heart J 1984; 52:178–85.

[5] Gomes AS. MR imaging of congenital anomalies of the thoracic aorta and pulmonary arteries. Radiol Clin North Am 1989;27:1171–81.

[6] Strouse PJ, Hernandez RJ, Beekman III RH. Assessment of central ventral pulmonary arteries in obstructive lesions of the right ventricle: comparison of magnetic resonance imaging and cine-angiography. Submitted to AJR 1996;167:1175–1183.

[7] Bisset GS III, Strife JL, Kirks DR, et al. Vascular rings: MR imaging. AJR 1987;149:251–6.

[8] Bank ER, Aisen AM, Rocchini AP, Hernandez RJ. Coarctation of the aorta in children undergoing angioplasty: pretreatment and posttreatment MR imaging. Radiology 1987;162:235–40.

[9] von Schulthess GK, Higashino SM, Higgins SS, Didier D, Fisher MR, Higgins CB. Coarctation of the aorta: MR imaging. Radiology 1986;158: 469–74.

[10] Fawzy ME, von Sinner W, Rifai A, Galal O, Dunn B, El-Deeb F, Zaman L. Magnetic resonance imaging compared with angiography in the evaluation of intermediate-term result of coarctation balloon angioplasty. Am Heart J 1993;126:1380–4.

[11] Bromberg BI, Beekman RH, Rocchini AP, Snider AR, Bank ER, Heidelberger K, Rosenthal A. Aortic aneurysm after patch aortoplasty repair of coarctation: a prospective analysis of prevalence, screening tests and risks. J Am Coll Cardiol 1989;14: 734–41.

[12] Julsrud PR, Breen JF, Felmlee JP, Warnes CA, Connolly HM, Schaff HV. Coarctation of the aorta: collateral flow assessment with phase-contrast MR angiography. AJR 1997;169:1735–42.

[13] Steffens JC, Bourne MW, Sakuma H, O'Sullivan M, Higgins CB. Quantification of collateral blood flow in coarctation of the aorta by velocity encoded cine magnetic resonance imaging. Circulation 1994; 90:937–43.

[14] Geva T, Vick III GW, Wendt RE, Rokey R. Role of spin echo and cine magnetic resonance imaging in presurgical planning of heterotaxy syndrome. Comparison with echocardiography and catheterization. Circulation 1994;90:348–56.

[15] Niwa K, Uchishiba M, Aotsuka H, Tateno S, Tasima K, Fujiwara T, Matsuo' K. K: Magnetic resonance imaging of heterotaxia in infants. JACC 1994;233:177–83.

[16] Julsrud PR, Ehman RL, Hagler DJ, Iistrup DM. Extracardiac vasculature in candidates for Fontan surgery: MR imaging. Radiology 1989;173:503–6.

[17] Choe YH, Lee HJ, Kim HS, Ko JK, Kim JE, Han JJ. MRI of total anomalous pulmonary venous connections. J Comput Asst Tomogr 1994;128: 243–9.

[18] Masui T, Seelos KC, Kersting-Sommerhioff BA, Higgins CB. Abnormalities of the pulmonary veins: evaluation with MR imaging and comparison with cardiac angiography and echocardiography. Radiology 1991;181:645–9.

[19] Ross RD, Bissett GS, Meyer RA, Hannon DW, Bove KE. Magnetic resonance imaging for diagnosis of pulmonary vein stenosis after "correction" of total anomalous pulmonary venous connection. Am J Cardiol 1987;60:1199–201.